Fabrication and characterization of a room-temperature ZnO polariton laser

Feng Li, L. Orosz, O. Kamoun, S. Bouchoule, C. Brimont et al.

Citation: Appl. Phys. Lett. **102**, 191118 (2013); doi: 10.1063/1.4804986
View online: http://dx.doi.org/10.1063/1.4804986
View Table of Contents: http://apl.aip.org/resource/1/APPLAB/v102/i19
Published by the American Institute of Physics.

Fabrication and characterization of a room-temperature ZnO polariton laser

Feng Li,[1,2] L. Orosz,[3] O. Kamoun,[4] S. Bouchoule,[5] C. Brimont,[4] P. Disseix,[3] T. Guillet,[4] X. Lafosse,[5] M. Leroux,[1] J. Leymarie,[3] G. Malpuech,[3] M. Mexis,[4] M. Mihailovic,[3] G. Patriarche,[5] F. Réveret,[3] D. Solnyshkov,[3] and J. Zuniga-Perez[1,a)]
[1]*CRHEA-CNRS, Rue Bernard Gregory, 06560 Valbonne, France*
[2]*Université de Nice Sophia-Antipolis, 06103 Nice, France*
[3]*Institut Pascal, PHOTON-N2, Clermont Université, CNRS and Université Blaise Pascal, 24 Avenue des Landais, 63177 Aubière cedex, France*
[4]*Université de Montpellier 2, CNRS, Laboratoire Charles Coulomb, UMR 5221, 34095 Montpellier, France*
[5]*LPN-CNRS, Route de Nozay, 91460 Marcoussis, France*

(Received 20 March 2013; accepted 27 April 2013; published online 16 May 2013)

A ZnO planar optical microcavity displaying room-temperature polariton lasing over a wide range of cavity-exciton detunings has been fabricated. The cavity combines optimum crystalline quality, given by a ZnO single-crystal substrate, and optimum photonic quality, obtained by the use of two dielectric SiO_2/HfO_2 Bragg mirrors. A maximum cavity quality factor of about 4000 has been measured. Typically, the polariton lasing transition is accompanied by an increase of the output intensity by more than two orders of magnitude, a reduction of the emission linewidth and a relatively small blueshift of the lower polariton branch (less than 5% of the Rabi splitting). © *2013 AIP Publishing LLC*. [http://dx.doi.org/10.1063/1.4804986]

Semiconductor planar microcavities operating in the strong-coupling regime, i.e., optical resonators in which the *eigenmodes* of the system are no longer purely excitonic or photonic but a mixture of them,[1] have seen a rapid development in the last years especially since the demonstration of polariton Bose-Einstein condensation.[2,3] The numerous and exciting discoveries that have followed, including superfluidity[4] and topological defects generation,[5] have been possible owing to a mature fabrication technology of distributed Bragg reflectors (DBR) and semiconductor heterostructures, mainly based on GaAs or CdTe. This evolution has finally led to polariton manipulation.[6,7] All these experiments were carried out at low temperatures because, even if the strong-coupling regime might be kept up to room temperature in these materials, their limited exciton stability at high temperatures and large particle densities precludes condensation at 300 K. In fact, if polariton condensation at the bottom of the lower polariton branch (LPB) needs to be obtained at room temperature, materials with larger oscillator strengths and larger exciton binding energy must be employed. This is the reason why much attention has been paid lately to organic semiconductors,[8] GaN[9–12] and ZnO.

While planar GaN microcavities have been largely studied since the late 1990s, given their applications in the solid-state lighting domain (including resonant cavity light-emitting diodes and vertical cavity surface emitting lasers), the first GaN cavity displaying the strong exciton-photon coupling regime at room-temperature was not reported until 2005.[9] Room-temperature polariton lasing was obtained in a bulk GaN cavity just two years later[10] and in 2008 in a quantum-well based structure.[12] The best figures of merit for these first room-temperature polariton lasers, as given by the cavity quality factor, Q-factor (which is proportional to the cavity photon lifetime), and the Rabi splitting, Ω_{Rabi} (which is a measure of the light-matter interaction inside the cavity), were about 1000 and 56 meV, respectively. However, since the polariton trap at the bottom of the LPB is roughly given by $\Omega_{Rabi}/2$,[13] and given that the thermal energy at room temperature is ~25 meV, optimized polariton lasers operating at room-temperature or above require larger Ω_{Rabi}.[14] In this context, the use of ZnO appears extremely interesting since, for a given cavity thickness, the Ω_{Rabi} scales as the square root of the exciton oscillator strength and the latter is four to eight times larger in ZnO than in GaN. Indeed, in ZnO cavities Ω_{Rabi} values of more than 200 meV should be attainable provided that the overlap between the exciton and the cavity modes is maximized.[15] Unfortunately, the exploitation of such large Ω_{Rabi} values requires the use of DBRs with stop-band widths larger than Ω_{Rabi}; otherwise, polaritons can relax towards LPBs associated with Bragg (leaky) modes whose lifetimes are much smaller than that of the cavity-associated LPB.[16] This limits the use of either ZnO/ZnMgO[17] or AlN/AlGaN[18,19] DBRs, which are in principle best suited for the epitaxial growth of the ZnO active region, but which exhibit stop-band widths going from about 200 meV to less than 300 meV. This drawback points towards the need of dielectric DBRs which, due to a much larger refractive index contrast, allow for larger stop band widths and, incidentally, larger absolute reflectivities (for the same number of DBR pairs) and larger Ω_{Rabi} (for the same cavity thickness) due to a smaller field penetration length into the DBRs. However, the deposition of the ZnO active layer onto an amorphous or polycrystalline DBR results in a multigrain ZnO active medium of degraded crystalline quality,[20] compared to the epitaxial approach.[17–19]

In this letter, we report on the fabrication and characterization of a ZnO-bulk microcavity solving the antagonism between epitaxial high-crystalline-quality ZnO active region and dielectric DBRs with large stop-band widths and high reflectivities.

a)Electronic mail: jzp@crhea.cnrs.fr

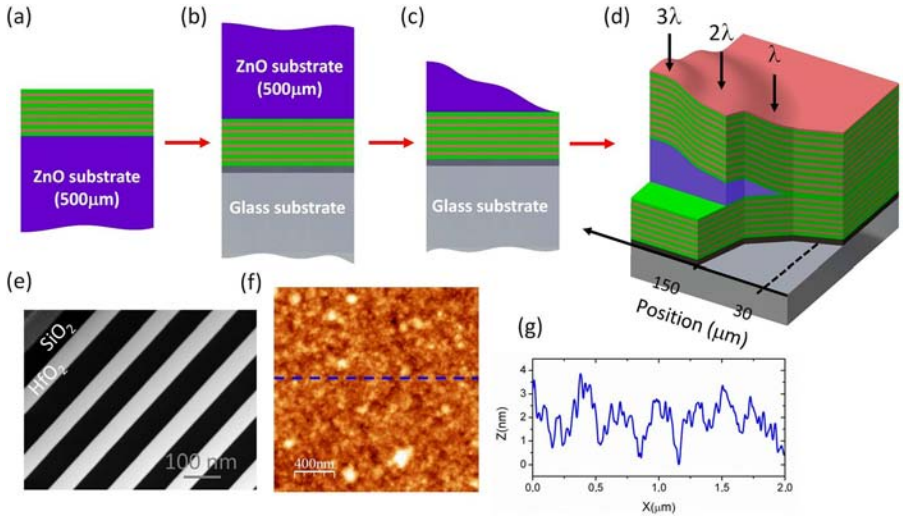

FIG. 1. Fabrication of the fully hybrid bulk ZnO microcavity. (a) A single-crystal *c*-ZnO substrate is covered by a HfO_2/SiO_2 DBR (6.5 pairs) completed by Al. (b) The whole DBR/ZnO substrate is flipped upside-down and transferred to a glass substrate. (c) The ZnO substrate is backside etched/polished down to a thickness of several tens to hundreds nanometers. (d) A HfO_2/SiO_2 DBR (10 pairs) is deposited on top of the processed ZnO substrate. (e) High-angle annular dark field scanning transmission electron microscopy image of a SiO_2/HfO_2 Bragg reflector as used in the cavity. (f) $2 \times 2\ \mu m^2$ atomic force microscopy image of the completed cavity (root mean squared roughness: 9 Å). (g) Height profile along the dashed line shown in (f).

The processing steps followed for the fabrication of the current cavity are illustrated in Figs. 1(a) to 1(d). First, a SiO_2/HfO_2 DBR (6.5 pairs) is deposited by ion-beam-assisted (Ar, O_2) electron-beam vacuum evaporation on top of a ZnO *c*-oriented substrate (Fig. 1(a)). The DBR is completed by the evaporation of a ~200-nm thick Al layer to achieve a nominal mirror reflectivity of ~99.8% at the Bragg wavelength ($\lambda \sim 380$ nm). The whole structure is then turned upside-down and transferred onto a host substrate (pyrex glass) using anodic bonding between Al and pyrex (Fig. 1(b)).[21] Next, the active layer is obtained by polishing/etching the 500-μm thick ZnO substrate down to a few hundreds of nanometers (Fig. 1(c)). A key-point of the process is that neither the ZnO optical quality (as shown later) nor its surface is degraded during the thinning. Indeed, the roughness of the ZnO surface after the final etching step is typically 5–10 Å in $2 \times 2\ \mu m^2$ atomic force microscopy images. Finally, the half-cavity is completed by a second SiO_2/HfO_2 DBR (10 pairs, see Fig. 1(d)), whose surface roughness reproduces that of the polished ZnO, as shown in Figs. 1(f) and 1(g). As schematically represented in Fig. 1(d), this fabrication approach results in a large active-layer thickness gradient that, as a consequence, leads to a large LPB-energy gradient (from about 0.5 meV/μm to about 10 meV/μm depending on the exact location on the wafer).[22] This allows to study polariton condensation or lasing[23] over a wide range of cavity-exciton detunings δ ($\delta = E_{Cav} - E_X$, with E_{Cav} and E_X being the uncoupled cavity and exciton modes, respectively), and over cavity optical thicknesses ranging from $\lambda/2$ to 5λ.

The combination of SiO_2 and HfO_2, with a relative refractive index contrast $(n_{High} - n_{Low})/(1/2(n_{High} + n_{Low}))$ of ~35% at a wavelength of 380 nm, results in measured stop-band widths in the order of 500 meV. This value is typically twice as large as the Rabi splitting of the current cavity (from about 180 meV to about 260 meV, depending on the exact cavity thickness)[22] thereby preventing any significant coupling between excitons and Bragg modes. As already stated, from the photonic point of view the main figure of merit of the cavity is its Q-factor, which was limited to about 500 for ZnO cavities grown on AlN/AlGaN DBRs[18,19] and to about 1000 in ZnO cavities employing two YSZ/Al_2O_3 DBRs grown by pulsed laser deposition.[20] Indeed, this was probably one of the limiting factors that prevented the observation of polariton lasing in ZnO cavities up to room-temperature. In the cavity described in this letter, the combination of SiO_2/HfO_2 DBRs and a reduced surface roughness leads to Qs in the order of 2000, with some spots exhibiting Qs up to 2600, as shown in Fig. 2(a). The experimental Qs

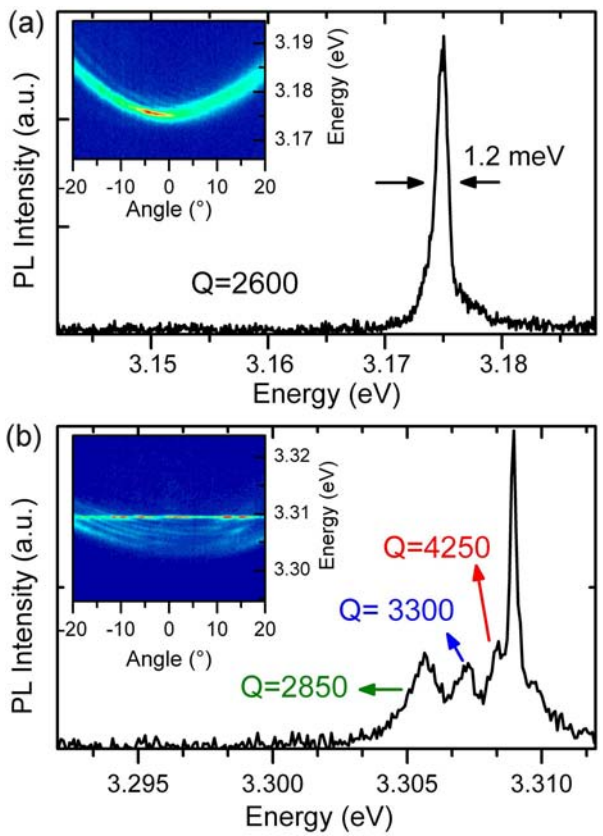

FIG. 2. Quality factor measurement with pulsed excitation (frequency-tripled Ti:Al_2O_3 laser with a repetition rate of 76 MHz and pulses duration of 130 fs). (a) μPL spectrum measured at an angle of 0° and T = 300 K below the polariton lasing threshold. The cavity thickness is 2.5 λ. The width at half maximum of the emission line is 1.2 meV. The inset shows the Fourier space image of the emission at the same location. (b) μPL spectrum measured at an angle of −10° and T = 5 K on another point of the sample just above the polariton lasing threshold. The widths of the individual modes can be extracted and are as small as 0.8 meV, corresponding to Q values of up to 4000. The inset shows the Fourier space image of the polariton emission at the same location. The presence of a series of discrete individual modes is clearly visible.

are smaller than the theoretical ones (Q = 5200 for a 2λ-thick cavity); one reason for this is that the measurement shown in Fig. 2(a) was carried out at a $\delta \sim 0$ meV, i.e., with an excitonic content close to 50%. Indeed, a proper measurement of Q would require a purely photonic mode (i.e., without any coupling to the exciton). However, the Ω_{Rabi} of the current ZnO cavity is so large that the coupling with excitons remains noticeable over the whole DBR stop band; thus, all our measurements suffer from an additional broadening due to the exciton-associated contribution. In Ref. 15, the authors estimated an exciton-induced broadening at room-temperature of about 2–3 meV for a 47% excitonic fraction polariton (a situation very close to ours in terms of δ). In view of our results, this estimation by Trichet *et al.* seems to be exceedingly large but it indicates, in any case, that the measured Q (2600) is a lower bound and that the actual Q may be much larger. Furthermore, even if the microPL measurements were performed with a laser spot size of 2 μm, the contribution of the polariton photonic fraction to the peak

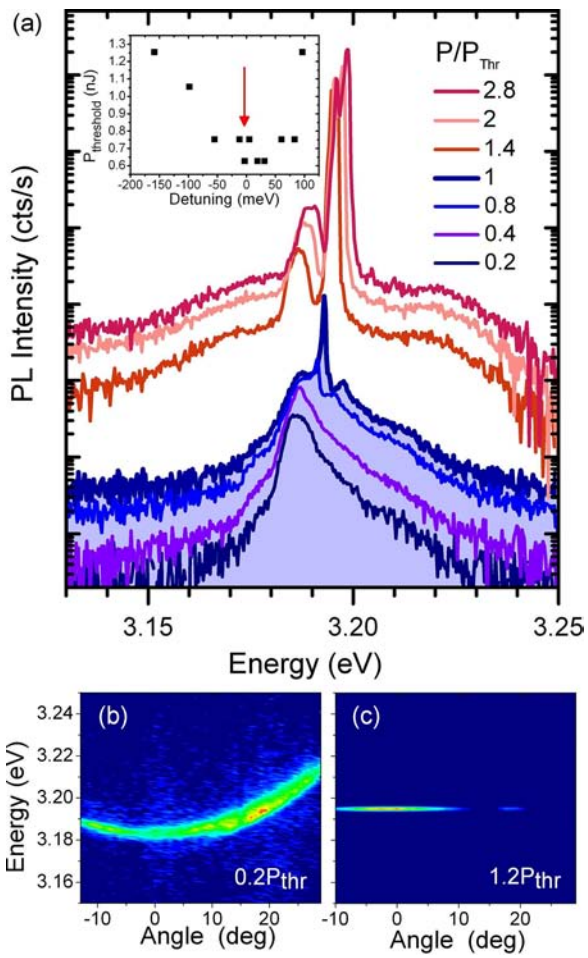

FIG. 3. Room-temperature polariton lasing. (a) Power dependent series of angle integrated μPL spectra measured at 300 K under quasi-continuous excitation (Nd:YAG laser with 4 kHz repetition rate and pulses of 400 ps, and a spot size of 2 μm). The excitation power relative to the threshold power is indicated for each spectrum. Inset: polariton lasing threshold at 300 K as a function of detuning. The arrow indicates the detuning at which the spectra in the main panels were obtained. Fourier space images (in linear scale) of the microcavity emission measured at 300 K and at the same point as in (a), under excitation power densities of $0.2P_{th}$ (b) and $1.2P_{th}$ (c), where $P_{th} = 0.6$ nJ/pulse is the polariton lasing threshold. At this point, the cavity optical thickness is 3λ, the Rabi splitting is 230 meV, and the detuning of the shown LPB is −8 meV.

width might not be purely of homogeneous nature and an inhomogeneous broadening contribution should be considered, especially taking into account the large thickness gradient of the active region. Indeed, by monitoring the emission just above threshold (see Fig. 2(b)), i.e., when the fraction of particles in the condensed state is low enough for still observing the dispersion of uncondensed polaritons, it is possible to resolve a series of discrete cavity modes that display equivalent dispersions but slightly different energies (whose origin is the large thickness gradient already discussed). In this case, Qs of several thousands can be measured, as shown in Fig. 2(b).

Such large Qs, the largest among room-temperature polariton lasers,[24] enable to achieve room-temperature polariton lasing in this ZnO cavity for a wide range of δ, as shown in the inset of Fig. 3. The minimum threshold is obtained for $\delta \sim 0$ meV,[22] which corresponds to cavity polaritons with an almost perfect 50% matter-50% light character, compared to an optimum $\delta \sim -50$ meV for a bulk-GaN polariton laser.[25] The difference for the optimum δ is explained by a much larger Ω_{Rabi} in our case, which is four times that of the GaN one and allows for a deeper polariton trap while maintaining a large excitonic fraction. The characteristics of the transition to the polariton laser regime are illustrated in Fig. 4 for δ close to the optimum, but at slightly more negative values, as indicated by the arrow in the inset of Fig. 3(a). At room-temperature, this transition is accompanied by a nonlinear increase of the output power (Fig. 4(b)), typically a factor 100 to 500 for less than 30% increase in the excitation power, and a reduction of the emission linewidth (Fig. 4(c)) well below the bare cavity mode linewidth, a clear signature of the onset of temporal coherence. An extremely important aspect to ensure that the cavity still operates in the strong-coupling regime above the nonlinear threshold, i.e., with no transition into the weak-coupling one,[26] is that the blueshift (Δ_{blue}) below threshold should be small compared to the actual Ω_{Rabi} and, especially, compared to the energy

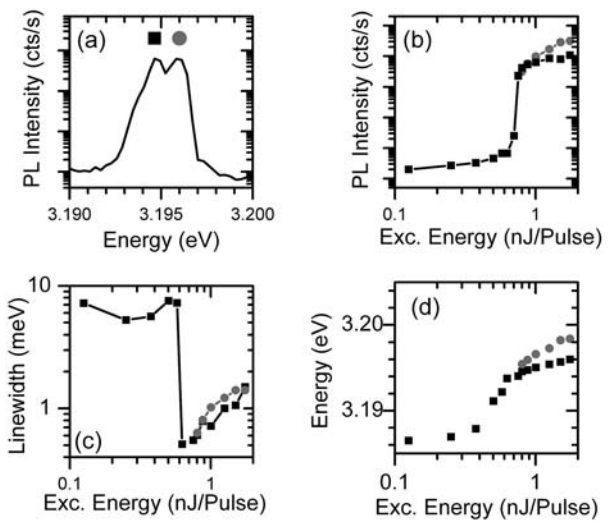

FIG. 4. Room temperature polariton lasing characteristics extracted from Fig. 3(a). (a) Detailed view around 3.195 eV of the spectrum at $1.4P_{th}$. For this power, and larger, two lasing modes, labelled by a square and by a circle symbols, can be resolved. (b) Integrated intensity, (c) linewidth, and (d) energy of the LPB/first lasing mode (square) and second lasing mode (circle), as a function of the excitation power.

difference between the bare cavity mode and the LPB (107 meV for the current position). In Fig. 4(d), these ratios amount to $\Delta_{blue}/\Omega_{Rabi} \sim 6\,meV/230\,meV \sim 3\%$ (at most 5% for any of the studied δ) and $\Delta_{blue}/(E_{Cav} - E_{LPB}) \sim 6\%$, which is much smaller than in previous reports.[27] These numbers ensure that lasing is occurring in the strong-coupling regime and, indeed, the bare cavity mode associated to the LPB monitored in Fig. 3 (and Fig. 4) is out of scale in Fig. 3(a).

The transition into a polariton lasing regime can occur under very different conditions considering the nature of the initial and final states (i.e., in equilibrium or out of equilibrium), and depends on the exact temperature and δ.[23,25] For the example used to illustrate it in the current letter, the out-of-equilibrium nature of the initial polariton gas reflects itself in the accumulation of polaritons, below threshold, at high energy and wavevectors different from zero (at an angle of about 20° in Fig. 3(b)). This situation is similar to that observed previously in GaAs cavities for sufficiently negative δ,[28] and which occurs when the LPB lifetime is shorter than the polariton relaxation time from the exciton reservoir to the bottom of the LPB. It should be noted that at more positive δ (e.g., $\delta \sim 100\,meV$ in the inset of Figure 3(a)), the LPB lifetime becomes larger and polaritons can relax down to the bottom of the LPB before condensation occurs. Finally, above threshold, and for excitation powers larger than 1.4 times the threshold power, multimode lasing is observed (for the point illustrated in Figs. 3 and 4), confirming the out-of-equilibrium character of the final condensate.[29]

To conclude, we have fabricated a ZnO optical microcavity displaying room-temperature polariton lasing by an innovative approach that combines the crystalline perfection of a ZnO bulk substrate and the optical superiority of UV-optimized dielectric mirrors. While this fabrication approach, and proposals in the same direction,[21] can be still improved (e.g., for controlling single-mode lasing), they open the way to large Q cavities displaying room-temperature polariton condensation as well as, subsequently, to manipulation of polariton condensates at room-temperature.

This work was partially supported by the EU under Contracts FP7 ITN Clermont4 (235114), Spin-Optronics (237252), and IRSES Polaphen (246912). The authors would like to acknowledge J. Y. Duboz for fruitful discussions.

[1]A. V. Kavokin, J. J. Baumberg, G. Malpuech, and F. P. Laussy, *Microcavities* (Oxford University Press, Great Clarendon Street, Oxford, 2007).
[2]J. Kazprzak, M. Richard, S. Kundermann, A. Baas, P. Jeambrun, J. M. J. Keeling, F. M. Marchetti, M. H. Szymanska, R. André, J. L. Staehli, V. Savona, P. B. Littlewood, B. Deveaud, and Le Si Dang, Nature **443**, 409 (2006).
[3]R. Balili, V. Hartwell, D. Snoke, L. Pfeiffer, and K. West, Science **316**, 1007 (2007).
[4]A. Amo, D. Sanvitto, F. P. Laussy, D. Ballarini, E. del Valle, M. D. Martin, A. Lemaître, J. Bloch, D. N. Krizhanovskii, M. S. Skolnick, C. Tejedor, and L. Viña, Nature **457**, 291 (2009).
[5]K. G. Lagoudakis, T. Ostatnicky, A. V. Kavokin, Y. G. Rubo, R. André, and B. Deveaud-Plédran, Science **326**, 974 (2009).
[6]E. Wertz, L. Ferrier, D. D. Solnyshkov, R. Johne, D. Sanvitto, A. Lemaître, I. Sagnes, R. Grousson, A. V. Kavokin, P. Senellart, G. Malpuech, and J. Bloch, Nat. Phys. **6**, 860–864 (2010).
[7]T. Gao, P. S. Eldridge, T. C. H. Liew, S. I. Tsintzos, G. Stavrinidis, G. Deligeorgis, Z. Hatzopoulos, and P. G. Savvidis, Phys. Rev. B **85**, 235102 (2012).
[8]S. Kéna-Cohen and S. R. Forrest, Nature Photon. **4**, 371 (2010).
[9]F. Semond, I. R. Sellers, F. Natali, D. Byrne, M. Leroux, J. Massies, N. ollier, J. Leymarie, P. Disseix, and A. Vasson, Appl. Phys. Lett. **87**, 021102 (2005).
[10]S. Christopoulos, G. Baldassarri Höger von Högersthal, J. J. Baumberg, A. J. D. Grundy, P. G. Lagoudakis, A. V. Kavokin, G. Christamnn, R. Butté, E. Feltin, J. F. Carlin, and N. Grandjean, Phys. Rev. Lett. **98**, 126405 (2007).
[11]J. J. Baumberg, A. V. Kavokin, S. Christopoulos, A. J. D. Grundy, R. Butté, G. Christamnn, D. D. Solnyshkov, G. Malpuech, G. Baldassarri Höger von Högersthal, E. Feltin, J. F. Carlin, and N. Grandjean, Phys. Rev. Lett. **101**, 136409 (2008).
[12]G. Christmann, R. Butté, E. Feltin, J. F. Carlin, and N. Grandjean, Appl. Phys. Lett. **93**, 051102 (2008).
[13]For a given Ω_{Rabi}, the actual depth of the polariton trap also depends on the cavity-exciton detuning (see Ref. 1).
[14]R. Johne, D. D. Solnyshkov, and G. Malpuech, Appl. Phys. Lett. **93**, 211105 (2008).
[15]A. Trichet, L. Sun, G. Pavlovic, N. A. Gippius, G. Malpuech, W. Xie, Z. Chen, M. Richard, and Le Si Dang, Phys. Rev. B **83**, 041302 (2011).
[16]S. Faure, C. Brimont, T. Guillet, T. Bretagnon, B. Gil, F. Médard, D. Lagarde, P. Disseix, J. Leymarie, J. Zúñiga-Pérez, M. Leroux, E. Frayssinet, J. C. Moreno, F. Semond, and S. Bouchoule, Appl. Phys. Lett. **95**, 121102 (2009).
[17]S. Halm, S. Kalusniak, S. Sadofev, H. J. Wünsche, and F. Henneberger, Appl. Phys. Lett. **99**, 181121 (2011).
[18]T. Guillet, M. Mexis, J. Levrat, G. Rossbach, C. Brimont, T. Bretagnon, B. Gil, R. Butté, N. Grandjean, L. Orosz, F. Réveret, J. Leymarie, J. Zúñiga-Pérez, M. Leroux, F. Semond, and S. Bouchoule, Appl. Phys. Lett. **99**, 161104 (2011).
[19]L. Orosz, F. Réveret, F. Médard, P. Disseix, J. Leymarie, M. Mihailovic, D. Solnyshkov, G. Malpuech, J. Zuniga-Perez, F. Semond, M. Leroux, S. Bouchoule, X. Lafosse, M. Mexis, C. Brimont, and T. Guillet, Phys. Rev. B **85**, 121201 (2012).
[20]H. Franke, C. Sturm, R. Schmidt-Grund, G. Wagner, and M. Grundmann, New. J. Phys. **14**, 013037 (2012).
[21]L. Orosz, F. Réveret, S. Bouchoule, J. Zuniga-Perez, F. Médard, J. Leymarie, P. Disseix, M. Mihailovic, E. Frayssinet, F. Semond, M. Leroux, M. Mexis, C. Brimont, and T. Guillet, Appl. Phys. Express **4**, 072001 (2011).
[22]F. Li, L. Orosz, O. Kamoun, S. Bouchoule, C. Brimont, P. Disseix, T. Guillet, X. Lafosse, M. Leroux, J. Leymarie, M. Mexis, M. Mihailovic, G. Patriarche, F. Réveret, D. Solnyshkov, J. Zuniga-Perez, and G. Malpuech, Phys. Rev. Lett. **110**, 196406 (2013).
[23]J. Kasprzak, D. D. Solnyshkov, R. André, L. S. Dang, and G. Malpuech, Phys. Rev. Lett. **101**, 146404 (2008).
[24]Qs of up to 6400 have been reported for GaN VCSEL cavities operating in the visible. See R. Butté, G. Christmann, E. Feltin, A. Castiglia, J. Levrat, G. Cosendey, A. Altoukhov, J. F. Carlin, and N. Grandjean, Proc. SPIE **7216**, 721619 (2009).
[25]R. Butté, J. Levrat, G. Christmann, E. Feltin, J. F. Carli, and N. Grandjean, Phys. Rev. B **80**, 233301 (2009).
[26]T. Guillet, C. Brimont, P. Valvin, B. Gil, T. Bretagnon, F. Médard, M. Mihailovic, J. Zúñiga-Pérez, M. Leroux, F. Semond, and S. Bouchoule, Appl. Phys. Lett. **98**, 211105 (2011).
[27]T. C. Lu, Y. Y. Lai, Y. P. Lan, S. W. Huang, J. R. Chen, Y. C. Wu, W. F. Hsieh, and H. Deng, Opt. Express **20**, 5530 (2012); Y. Y. Lai, Y. P. Lan, and T. C. Lu, Appl. Phys. Express **5**, 082801 (2012).
[28]E. Wertz, L. Ferrier, D. Solnyshkov, P. Senellart, D. Bajoni, A. Maird, A. Lemaître, G. Malpuech, and J. Bloch, Appl. Phys. Lett. **95**, 051108 (2009).
[29]D. N. Krizhanovskii, K. G. Lagoudakis, M. Wouters, B. Pietka, R. A. Bradley, K. Guda, D. M. Whittaker, M. S. Skolnick, B. Deveaud-Plédran, M. Richard, R. André, and Le Si Dang, Phys. Rev. B **80**, 045317 (2009).